Electronic Supplementary Material (ESI) for Chemical Science.
This journal is © The Royal Society of Chemistry 2014

Electronic Supplementary Information for

Tunable Electrical Conductivity in Oriented Thin Films of Tetrathiafulvalene-Based Covalent Organic Framework

Song-Liang Cai,[†ab] Yue-Biao Zhang,[†cd] Andrew B. Pun,[a] Bo He,[a] Jinhui Yang,[de] Francesca M. Toma,[ef] Ian D. Sharp,[eg] Omar M. Yaghi,[cd] Jun Fan,[b] Sheng-Run Zheng,[b] Wei-Guang Zhang[b]* and Yi Liu[a]*

[a]The Molecular Foundry, Lawrence Berkeley National Laboratory, Berkeley, California 94720, United States

[b]School of Chemistry and Environment, South China Normal University, Guangzhou 510006, P. R. China

[c]Department of Chemistry, University of California–Berkeley, and Kavli Energy NanoSciences Institute at Berkeley, Berkeley, California 94720, United States

[d]Joint Center for Artificial Photosynthesis, [e]Material Sciences Division, [f]Chemical Sciences Division, [g]Physical Biosciences Division, Lawrence Berkeley National Laboratory, Berkeley, California 94720, United States

X-ray single-crystal structure analyses: Suitable single crystals of compounds **1** and **2** were selected under an optical microscope and quickly coated with epoxy before being mounted on a glass fiber for data collection. Data for them were collected on a Bruker APEX II CCD diffractometer equipped with a silicon 111 monochromator (T = 100 K, k = 0.7749 Å) on Station 11.3.1 at the ALS using synchrotron radiation.[1] Structure solutions were solved by direct methods[4, 5] and refined with the full-matrix least-squares methods on F^2.[2, 3] All non-hydrogen atoms were refined anisotropically, and all the hydrogen atom positions were fixed geometrically at calculated distances and allowed to ride on the parent atoms. Details of the crystal parameters, data collections, and refinements are summarized in Table S**1**. Crystallographic information files (CIFs) were deposited in Cambridge structural database, with Cambridge Crystallographic Data Center (CCDC) numbers 1001673-1001674 for compounds **1−2**, respectively.

Table S1. Crystallographic data and structure refinement summary for compounds **1** and **2**.

Compound	**1**	**2**
Empirical formula	$C_{34}H_{20}O_4S_4$	$C_{65}H_{48}N_4S_4$
Formula weight	620.74	1013.31
Wavelength (Å)	0.7749	0.7749
Crystal system	Triclinic	Monoclinic
Space group	P -1	P 21
a / Å	9.0590(12)	15.9142(7)
b / Å	11.3961(16)	7.9235(4)
c / Å	15.780(2)	20.8037(10)
α / °	68.8889(16)	90
β / °	79.0989(17)	106.326(3)
γ / °	67.1611(16)	90
V / Å^3	1398.3(3)	2517.5(2)
Z	2	2
D / g cm^{-3}	1.474	1.337
μ / mm^{-1}	0.477	0.295
F (000)	640	1060
T / K	100(2)	100(2)
Crystal size / mm	0.150 x 0.100 x 0.030	0.160 x 0.060 x 0.010
θ Range for data collection / (°)	2.664 – 33.641	2.064 – 33.663
Max., min. transmission	0.986, 0.882	0.997, 0.757
Reflections collected	19981	37054
Unique reflections	8355	13909
Number of parameters	379	715
R_{int}	0.0476	0.0487
Final *R* indices [$I > 2\sigma(I)$]	$R_1 = 0.0554$, $wR_2 = 0.1761$	$R_1 = 0.0557$, $wR_2 = 0.1379$
R indices (all data)	$R_1 = 0.0640$, $wR_2 = 0.1875$	$R_1 = 0.0780$, $wR_2 = 0.1511$
Goodness-of-fit	1.071	1.017

$R_1 = \sum||F_0| - |F_c|| / \sum|F_0|$, $wR_2 = \{\sum[w(F_0^2 - F_c^2)^2] / \sum(F_0^2)^2\}^{1/2}$

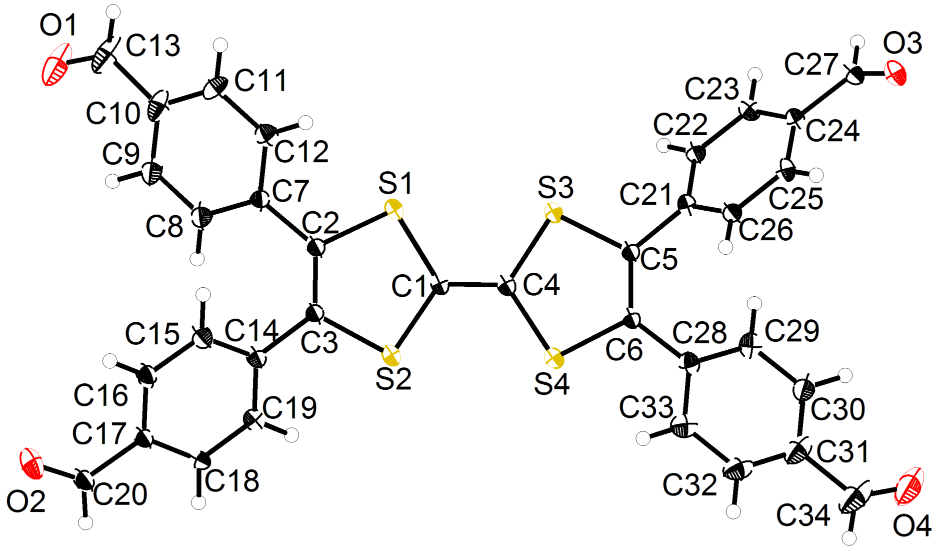

Figure S1. ORTEP drawing of the crystal structure of compound **1** (50% thermal ellipsoids).

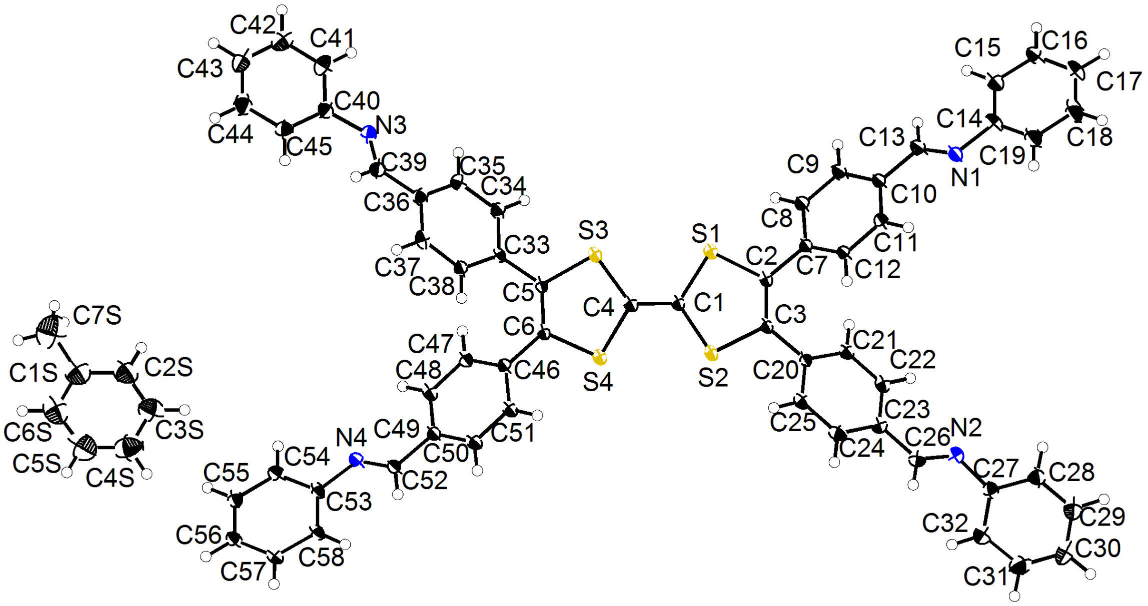

Figure S2. ORTEP drawing of the crystal structure of compound **2** (50% thermal ellipsoids).

Section S2. *Fourier-transform infrared (FT-IR) spectra*.

The FT-IR spectra of starting materials, analog compound, TTF-COF, I_2-doped TTF-COF, TCNQ, and TCNQ-doped TTF-COF were determined on a Perkin Elmer Spectrum One FT-IR Spectrometer with KBr pellets in the 400−4000 cm^{-1} region.

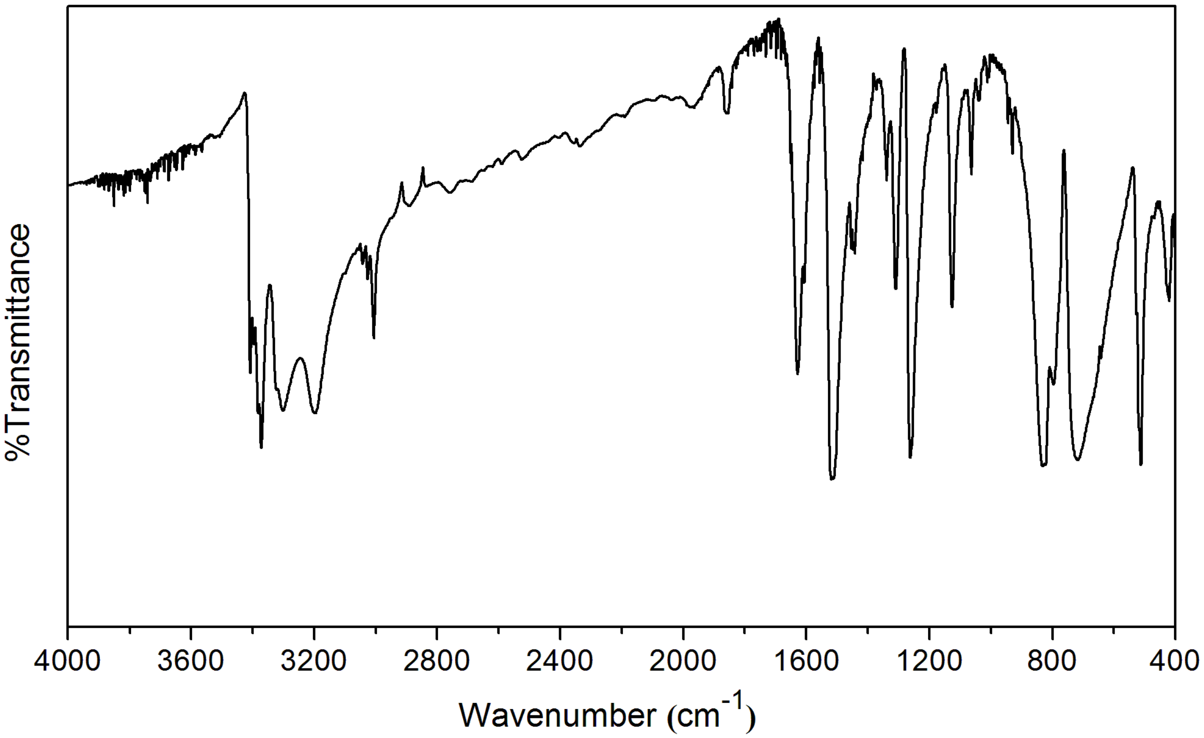

Figure S3. FT-IR spectrum of 1,4-diaminobenzene (**DAB**).

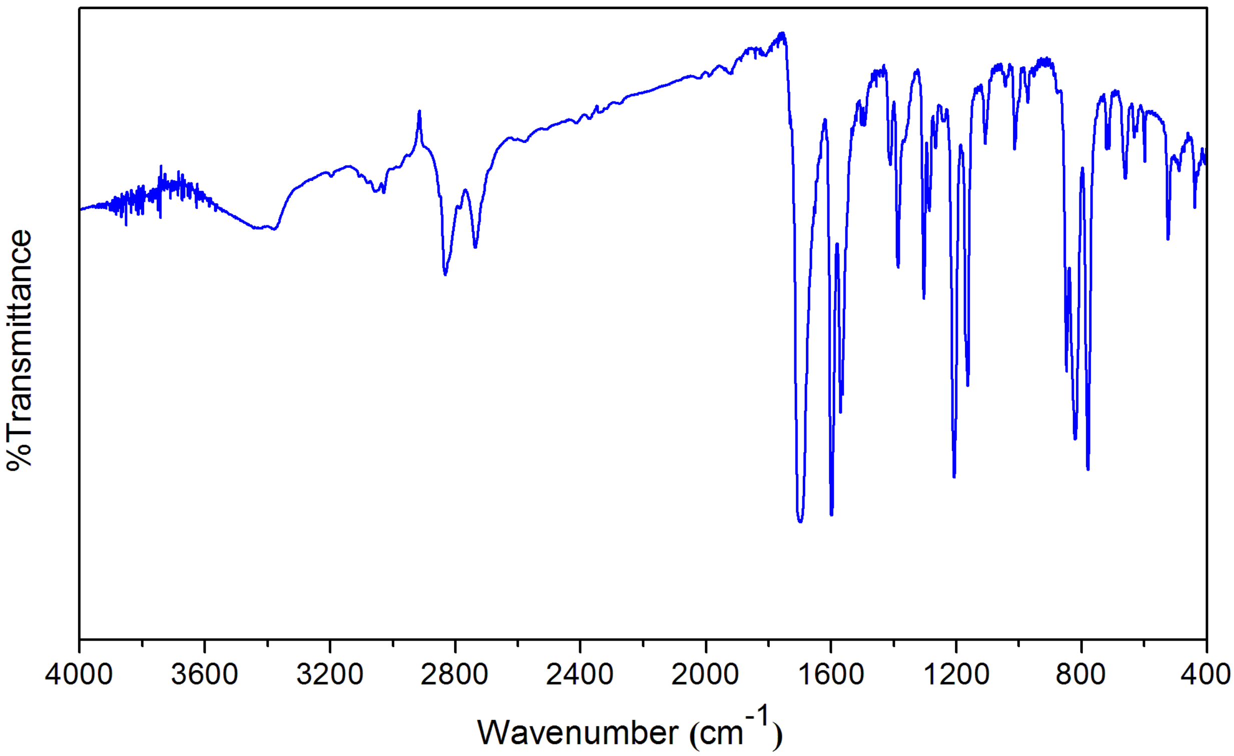

Figure S4. FT-IR spectrum of TTF tetrabenzaldehyde (**1**).

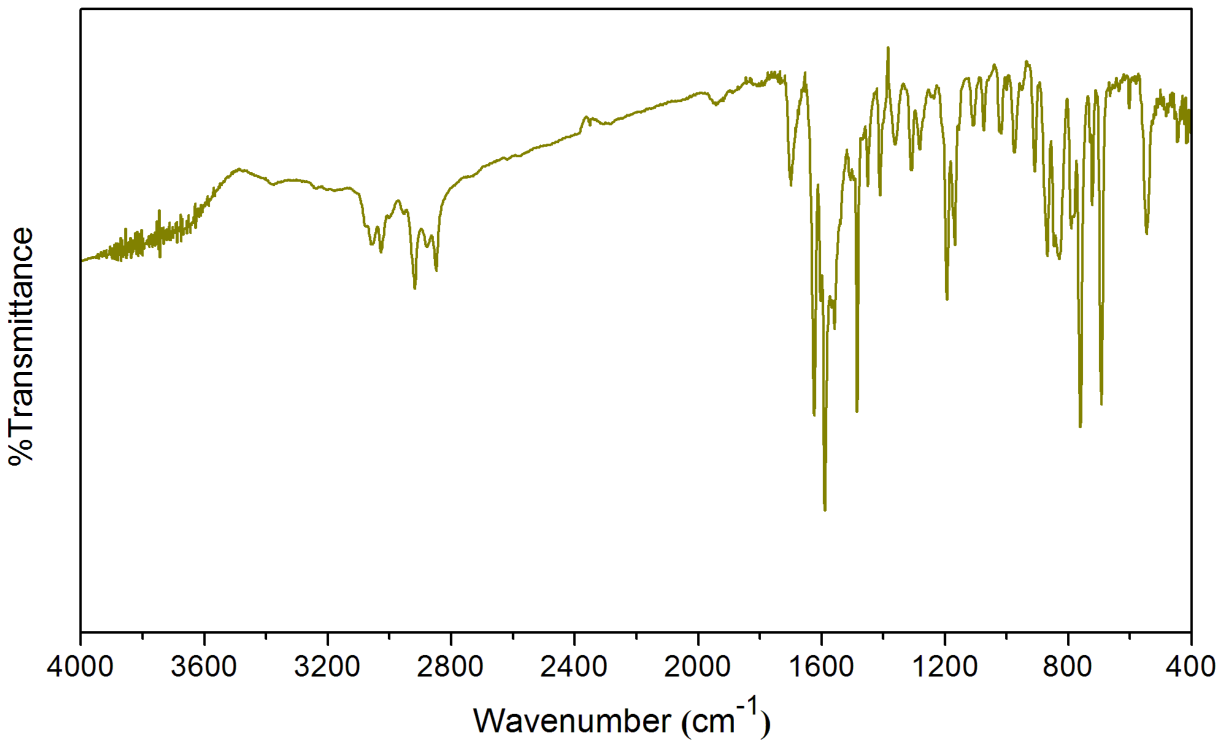

Figure S5. FT-IR spectrum of the “monomeric” analog compound tetraimino-TTF (**2**).

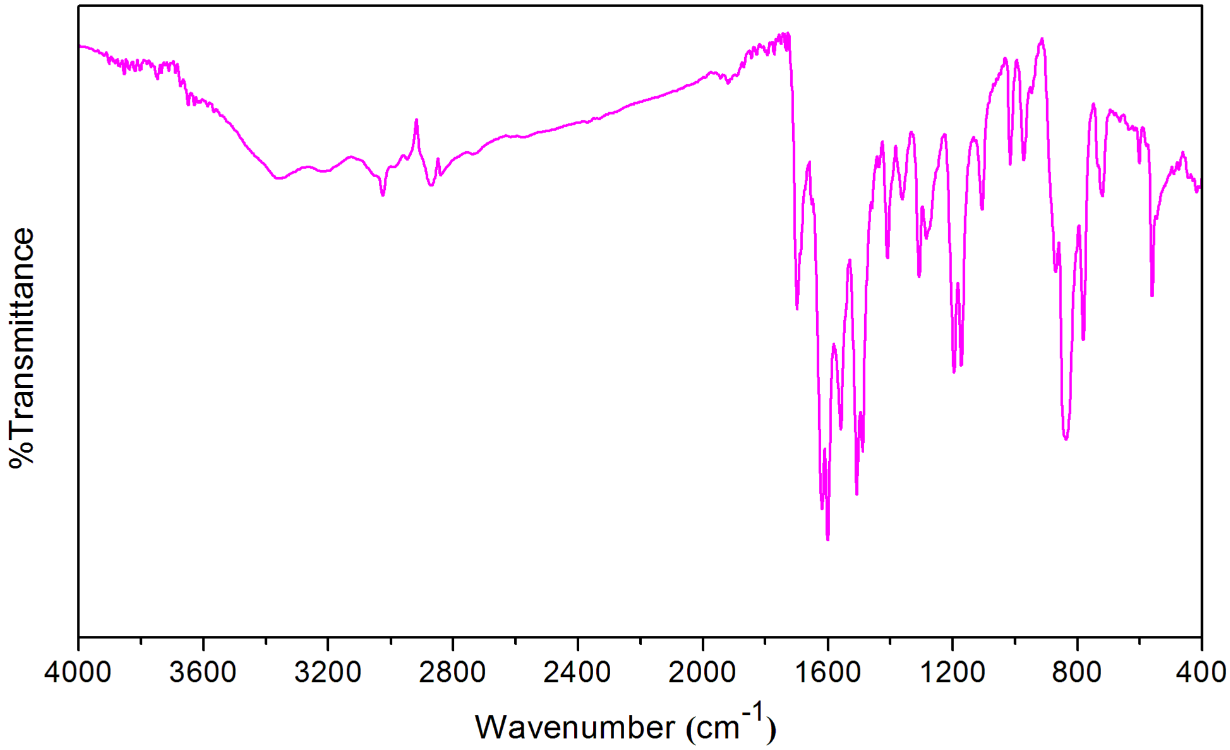

Figure S6. FT-IR spectrum of TTF-COF.

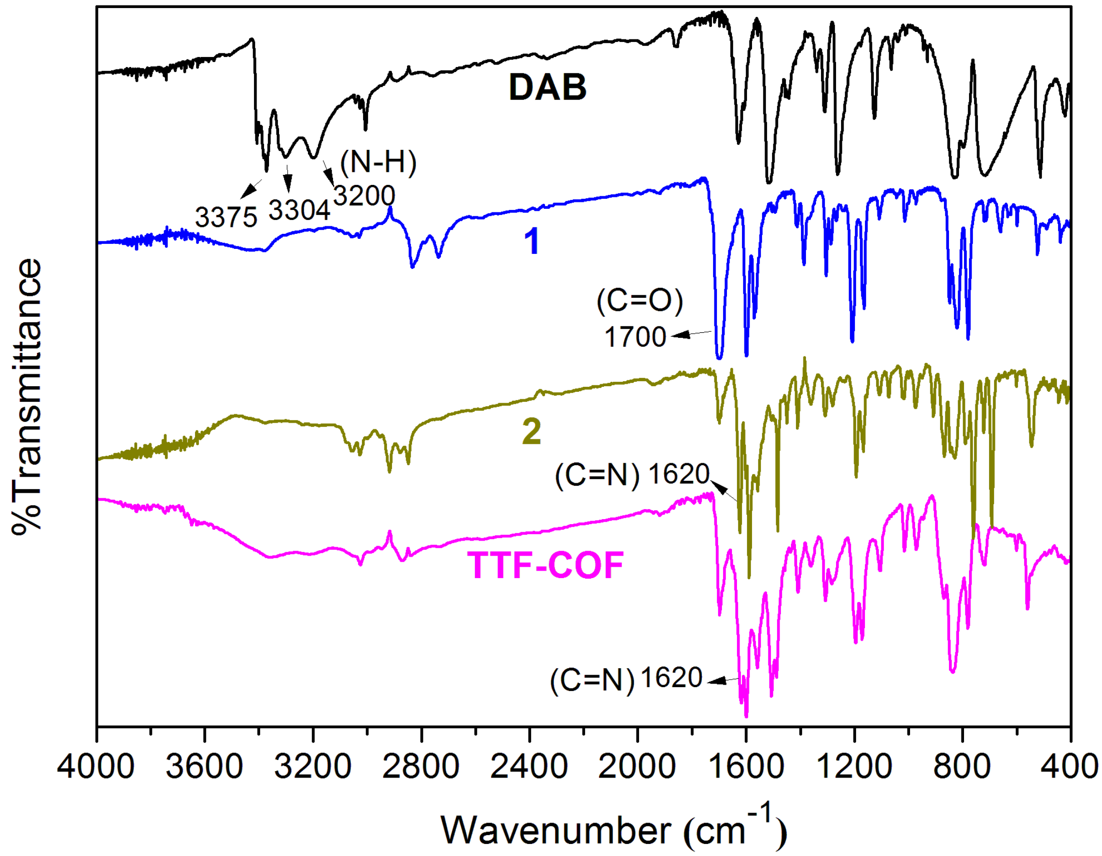

Figure S7. Stack plot of the FT-IR spectra for the comparison between starting materials, analog compound, and TTF-COF.

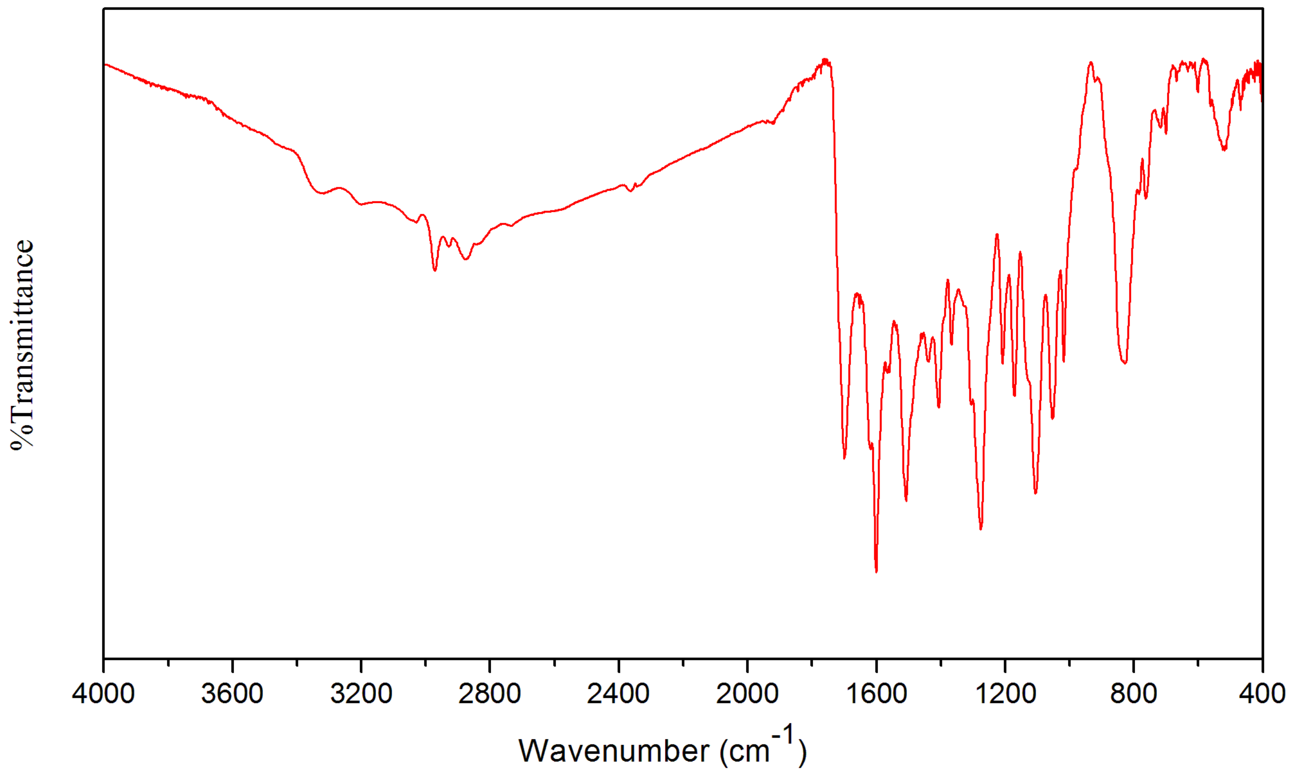

Figure S8. FT-IR spectrum of I_2-doped TTF-COF.

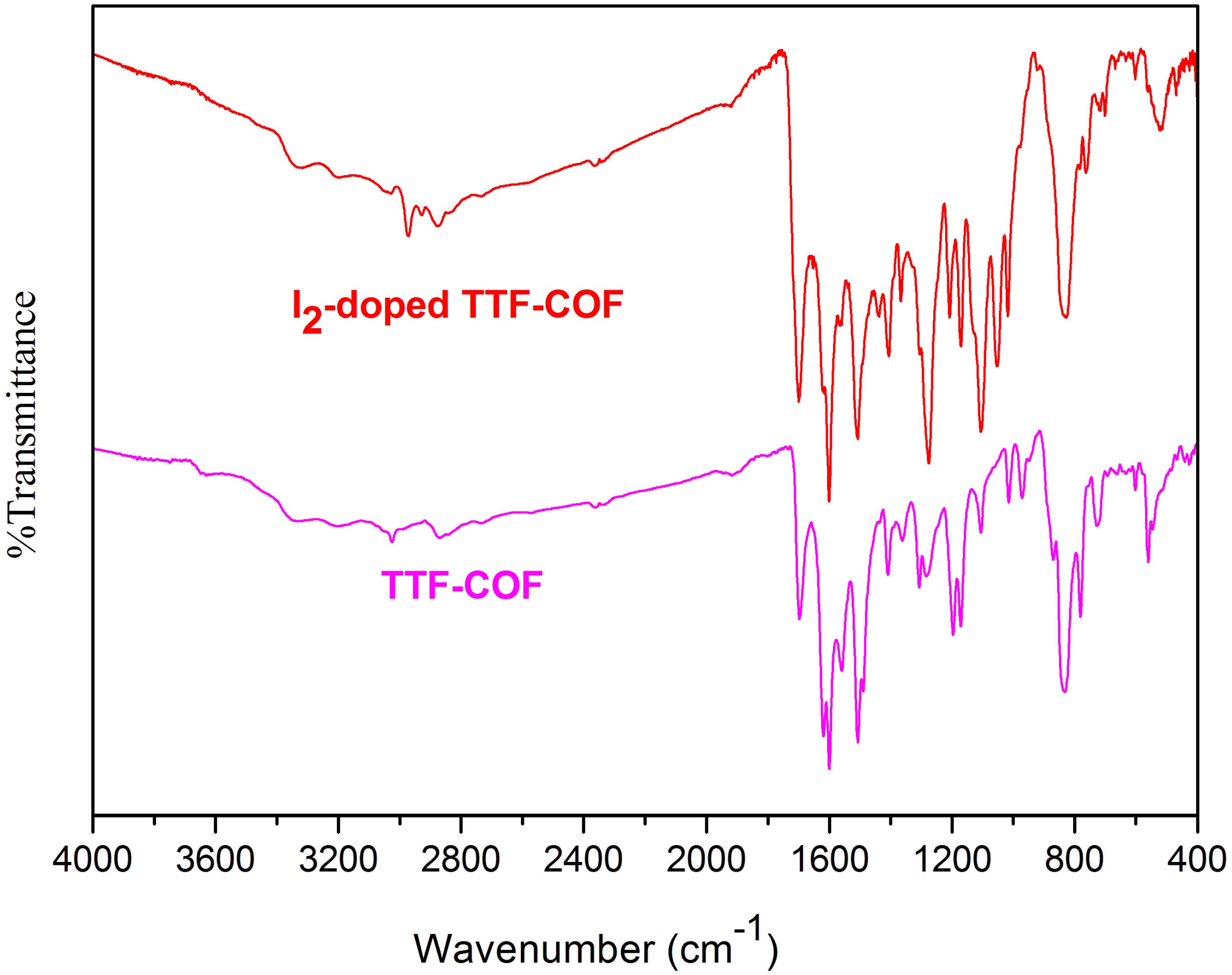

Figure S9. Stack plot of the FT-IR spectra for the comparison between TTF-COF and I_2-doped TTF-COF.

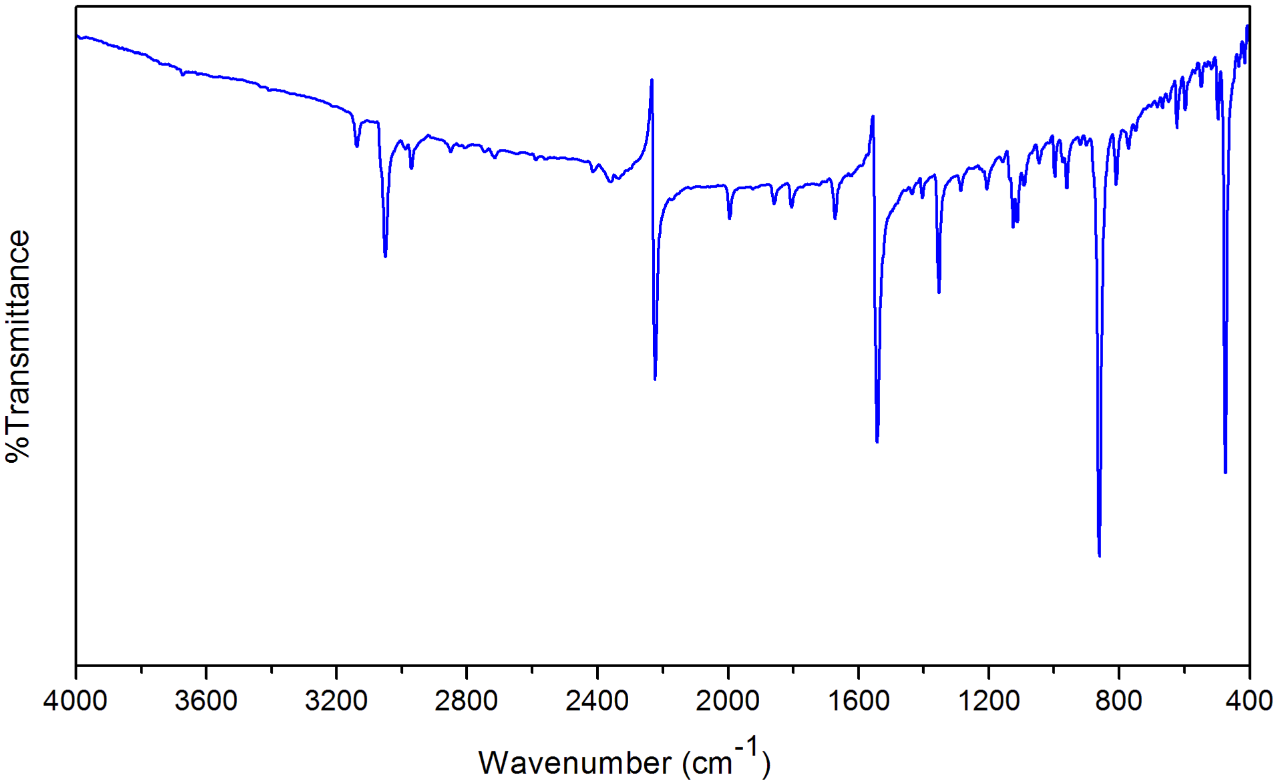

Figure S10. FT-IR spectrum of TCNQ.

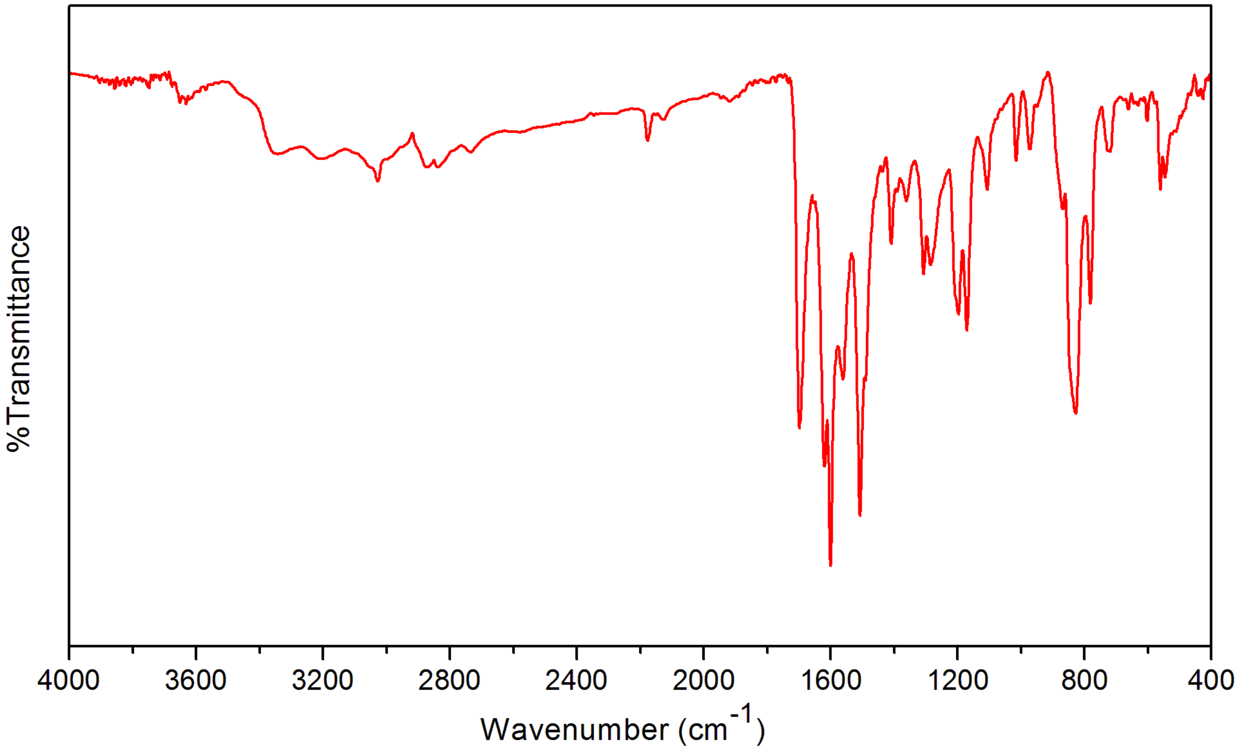

Figure S11. FT-IR spectrum of TCNQ-doped TTF-COF.

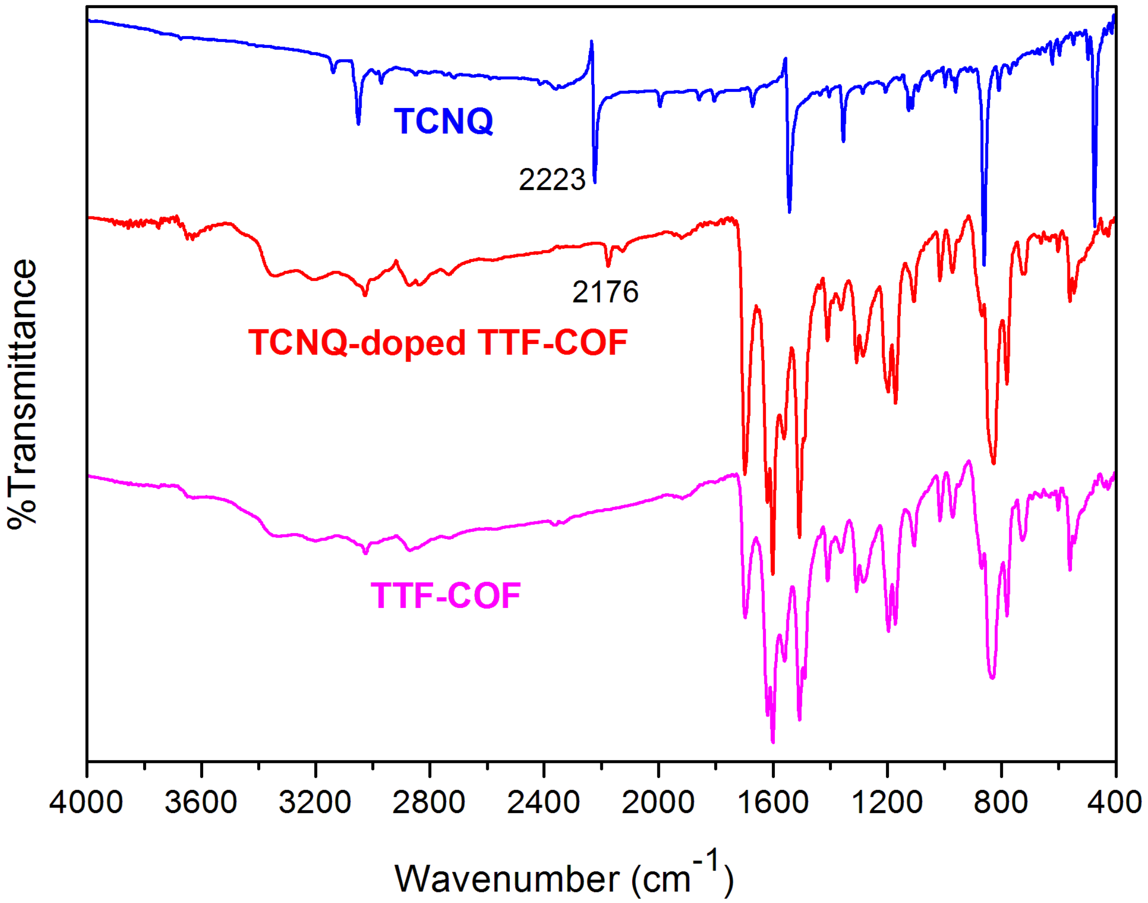

Figure S12. Stack plot of the FT-IR spectra for the comparison between TCNQ, TTF-COF and TCNQ-doped TTF-COF.

Section S3. *Solid-state nuclear magnetic resonance (SSNMR) spectroscopy*.

The solid-state nuclear magnetic resonance (SSNMR) spectrum was collected on a Bruker AV-500 NMR spectrometer using a standard Bruker magic angle-spinning (MAS) probe with 4-mm (o.d.) zirconia rotors. The magic angle was adjusted by maximizing the number and amplitudes of the signals of the rotational echoes observed in the ^{79}Br MAS FID signal from KBr. The transmitter frequnce of ^{13}C NMR is 125.80 MHz.

The spectrum was acquired using cross-polarization (CP) MAS technique with the ninety degree pulse of ^{1}H with 4.2 μs pulse width. The CP contact time was 2 ms. High power two-pulse phase modulation (TPPM) ^{1}H decoupling was applied during data acquisition. The decoupling frequency corresponded to 32 kHz. The MAS sample spinning rates varied from 8 to 13.5 kHz. Recycle delays between scans were 2 s. The ^{13}C chemical shifts are given relative to neat tetramethylsilane as zero ppm, calibrated using the methylene carbon signal of adamantane assigned to 38.48 ppm as secondary reference.[4]

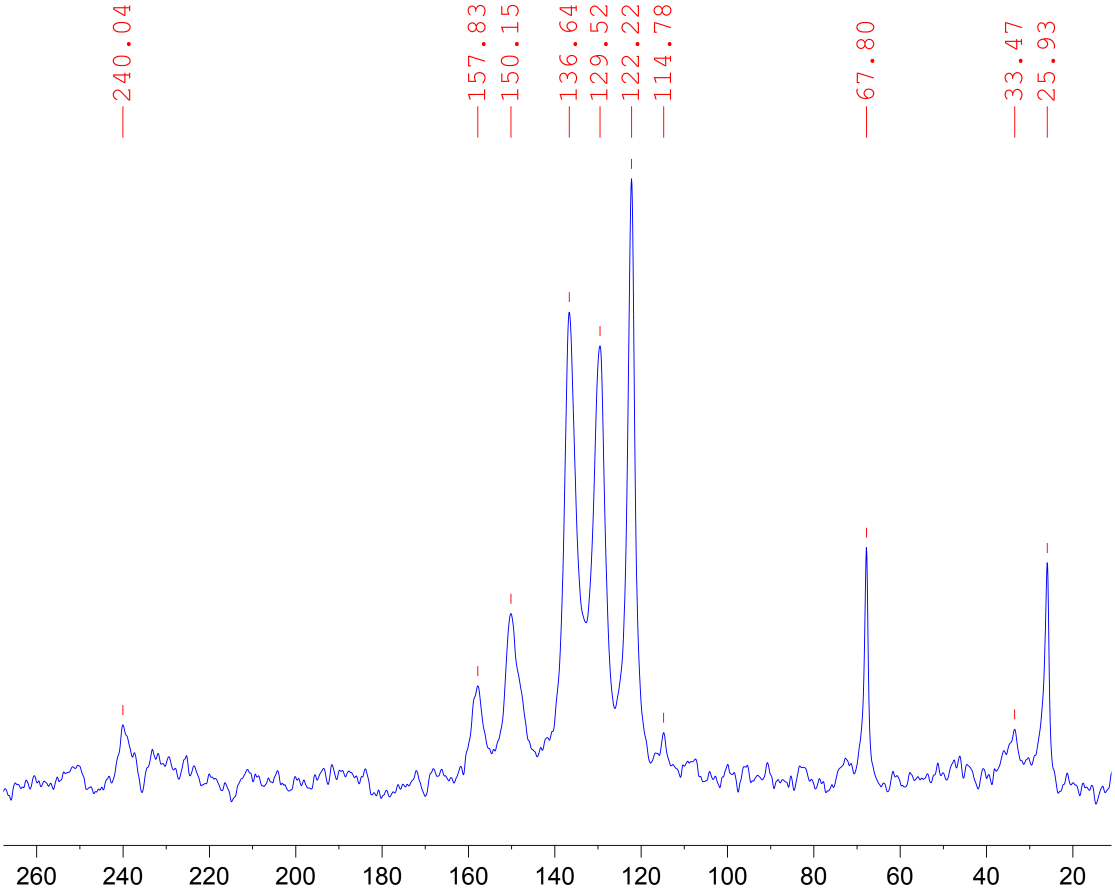

Figure S13. Solid state ^{13}C NMR of TTF-COF. The two humps at 240 and 33 ppm are spin side bands, and the two peaks at 67.8 and 25.9 ppm are from residue THF solvent.

Section S4. *Scanning electron microscopy (SEM).*

Scanning electron microscopy (SEM) image was recorded on a Zeiss Gemini Ultra-55 Analytical Scanning Electron Microscope using a beam energy of 5 kV and an In-Lens detector.

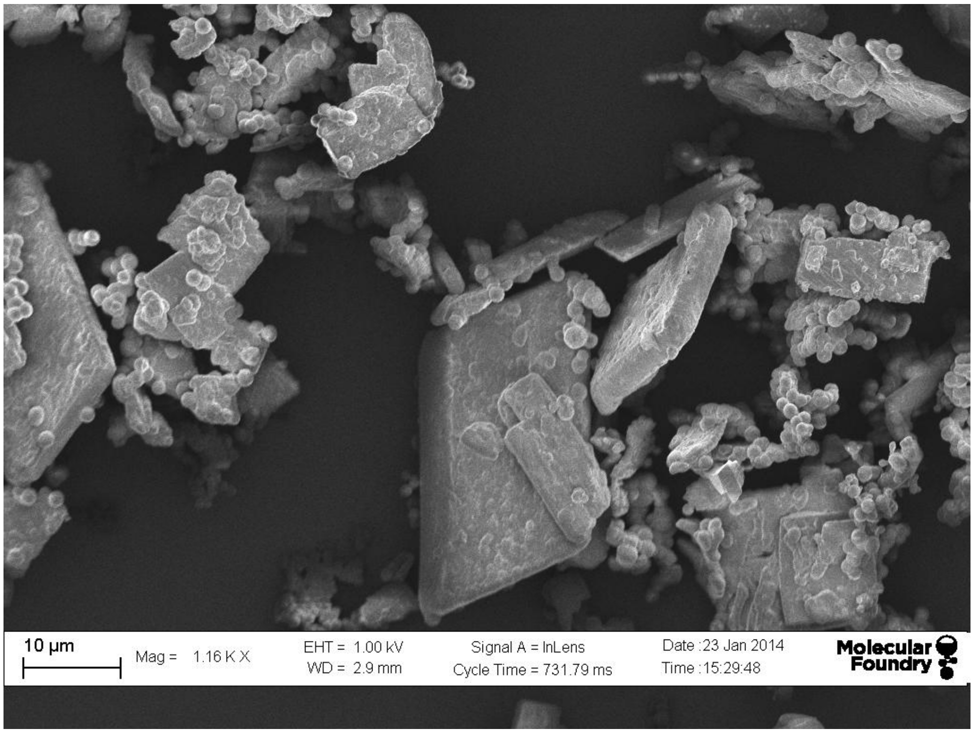

Figure S14. SEM image of TTF-COF.

***Section S5**. Crystal structure modeling and powder X-ray diffraction (PXRD) analyses.*

The crystal models for TTFCOF including the cell parameters and the atomic positions were generated by using Materials Studio 5.0 software package.[5] Atomic coordinates of TTF-COF crystal structure model are illustrated in Table S**2**.

Table S2. Fractional atomic coordinates for the unit cell of TTF-COF.

<table>
<tr><td colspan="4">TTF-COF</td></tr>
<tr><td colspan="4">Space group: <i>P4/MMM</i> (No. 123)
$a = b = 34.1585$ Å; $c = 3.5436$ Å
$\alpha = \beta = \gamma = 90°$
$V = 4135$ Å^3
$Z = 4$</td></tr>
<tr><td>Atom</td><td><i>x</i>/<i>a</i></td><td><i>y</i>/<i>b</i></td><td><i>z</i>/<i>c</i></td></tr>
<tr><td>C1</td><td>0.479400</td><td>1.000000</td><td>0.000000</td></tr>
<tr><td>C2</td><td>0.408140</td><td>0.979090</td><td>0.000000</td></tr>
<tr><td>S3</td><td>0.453720</td><td>0.957540</td><td>0.000000</td></tr>
<tr><td>C4</td><td>0.374480</td><td>0.950330</td><td>0.000000</td></tr>
<tr><td>C5</td><td>0.383040</td><td>0.909920</td><td>0.000000</td></tr>
<tr><td>C6</td><td>0.334880</td><td>0.960660</td><td>0.000000</td></tr>
<tr><td>C7</td><td>0.305060</td><td>0.932590</td><td>0.000000</td></tr>
<tr><td>C8</td><td>0.353690</td><td>0.881560</td><td>0.000000</td></tr>
<tr><td>C9</td><td>0.314520</td><td>0.892780</td><td>0.000000</td></tr>
<tr><td>C10</td><td>0.284490</td><td>0.862220</td><td>0.000000</td></tr>
<tr><td>N11</td><td>0.247380</td><td>0.870190</td><td>0.000000</td></tr>
<tr><td>C12</td><td>0.218190</td><td>0.840060</td><td>0.000000</td></tr>
<tr><td>C13</td><td>0.228570</td><td>0.800290</td><td>0.000000</td></tr>
<tr><td>C14</td><td>0.178560</td><td>0.850430</td><td>0.000000</td></tr>
<tr><td>H15</td><td>0.414770</td><td>0.899580</td><td>0.000000</td></tr>
<tr><td>H16</td><td>0.326030</td><td>0.992840</td><td>0.000000</td></tr>
<tr><td>H17</td><td>0.273100</td><td>0.942200</td><td>0.000000</td></tr>
<tr><td>H18</td><td>0.361770</td><td>0.849180</td><td>0.000000</td></tr>
<tr><td>H19</td><td>0.293410</td><td>0.830060</td><td>0.000000</td></tr>
<tr><td>H20</td><td>0.260750</td><td>0.791440</td><td>0.000000</td></tr>
<tr><td>H21</td><td>0.169730</td><td>0.882620</td><td>0.000000</td></tr>
</table>

Powder X-ray diffraction data collection. Powder X-ray diffraction (PXRD) was measured on a Bruker Gadds-8 diffractometer with a Cu-Kα source operating at 40 kV and 20 mA. Powder X-ray diffraction data were collected using a Bruker D8-advance θ-θ diffractometer in parallel beam geometry employing Cu Kα line focused radiation at 1600 W (40 kV, 40 mA) power and equipped with a position sensitive detector with at 6.0 mm radiation entrance slit. Samples were mounted on zero background sample holders by dropping powders from a wide-blade spatula and then leveling the sample with a razor blade. For the THF exchanged sample, an air-tight sample holder was employed to avoid solvent evaporation during the data acquisition. The best counting statistics were achieved by collecting samples using a 0.02º 2θ step scan from 1 – 50º with exposure time of 5 s per step. The Pawley PXRD refinement was performed using the Reflex module in the Materials Studio 5.0, in which a Pseudo-Voigt profile function was used for the profile fitting (peak broadening, peak asymmetry, and zero shift error were taken into account). Unit cell and sample parameter were refine simultaneously.

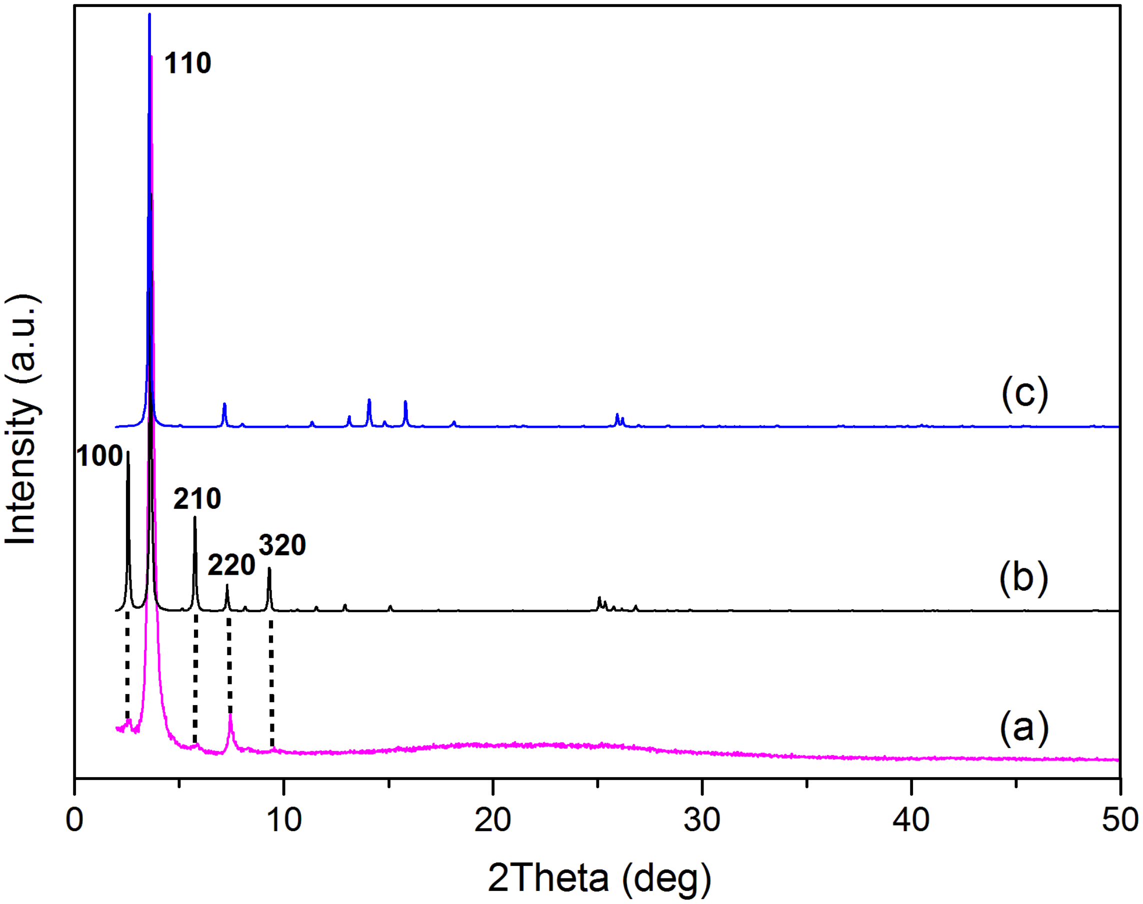

Figure S15. (a) Experimental PXRD pattern of TTF-COF; (b) Simulated PXRD pattern for the AA packing structure; (c) Simulated PXRD pattern for the AB packing structure.

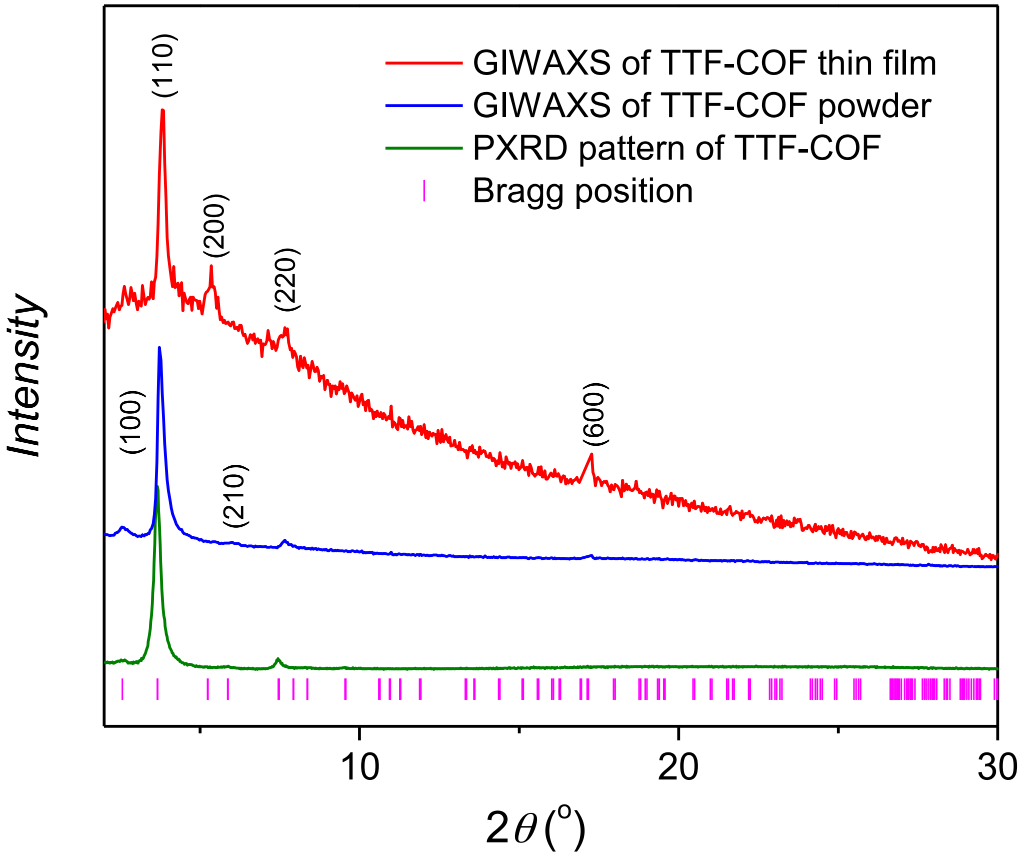

Figure S16. Comparison of Powder XRD (green) with the GIWAXS patterns of TTF-COF thin film (red) and powder (blue) samples. The purple sticks represent Bragg positions.

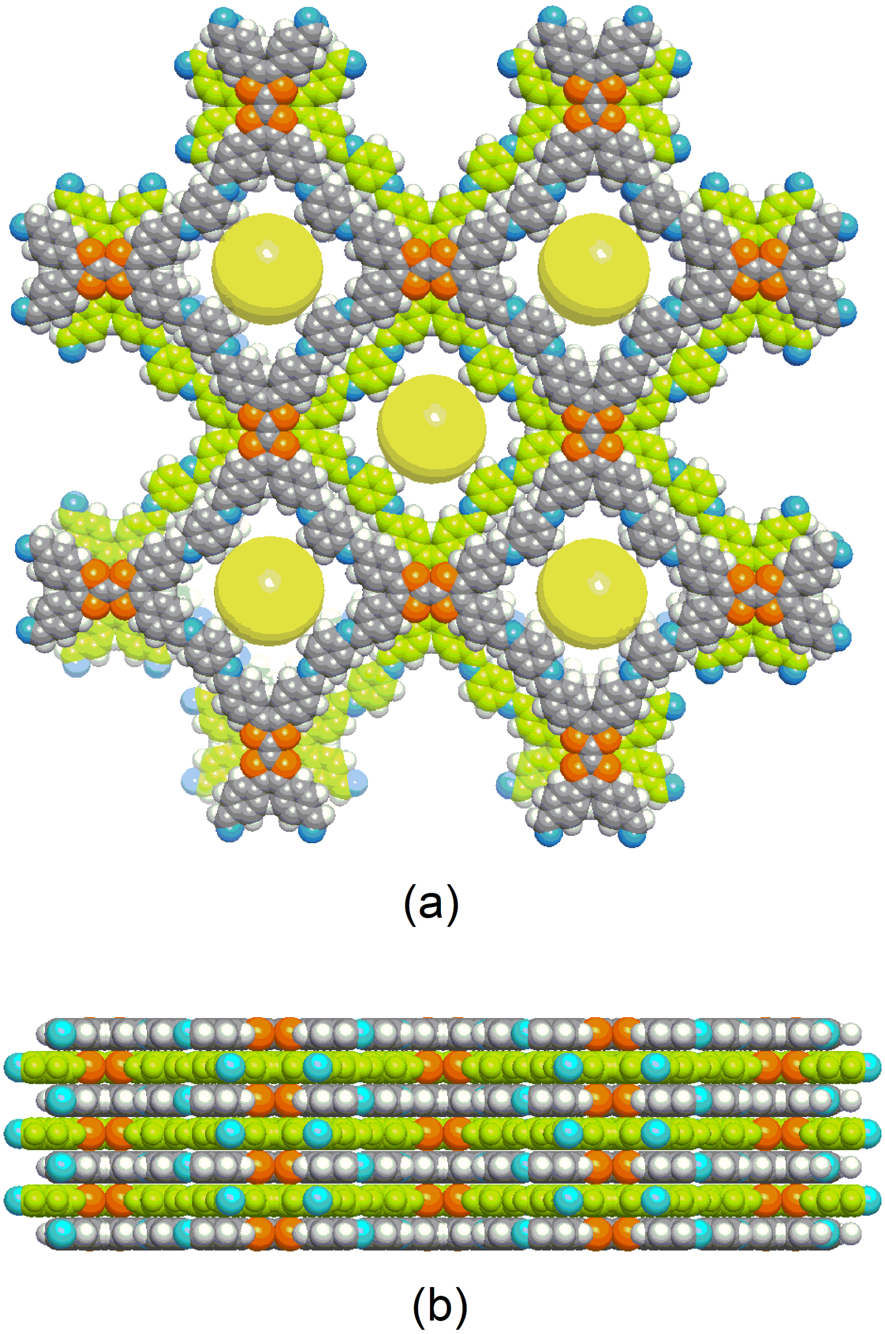

Figure S17. (a) Top and (b) side view of the AB packing structure of 2D TTF-COF.

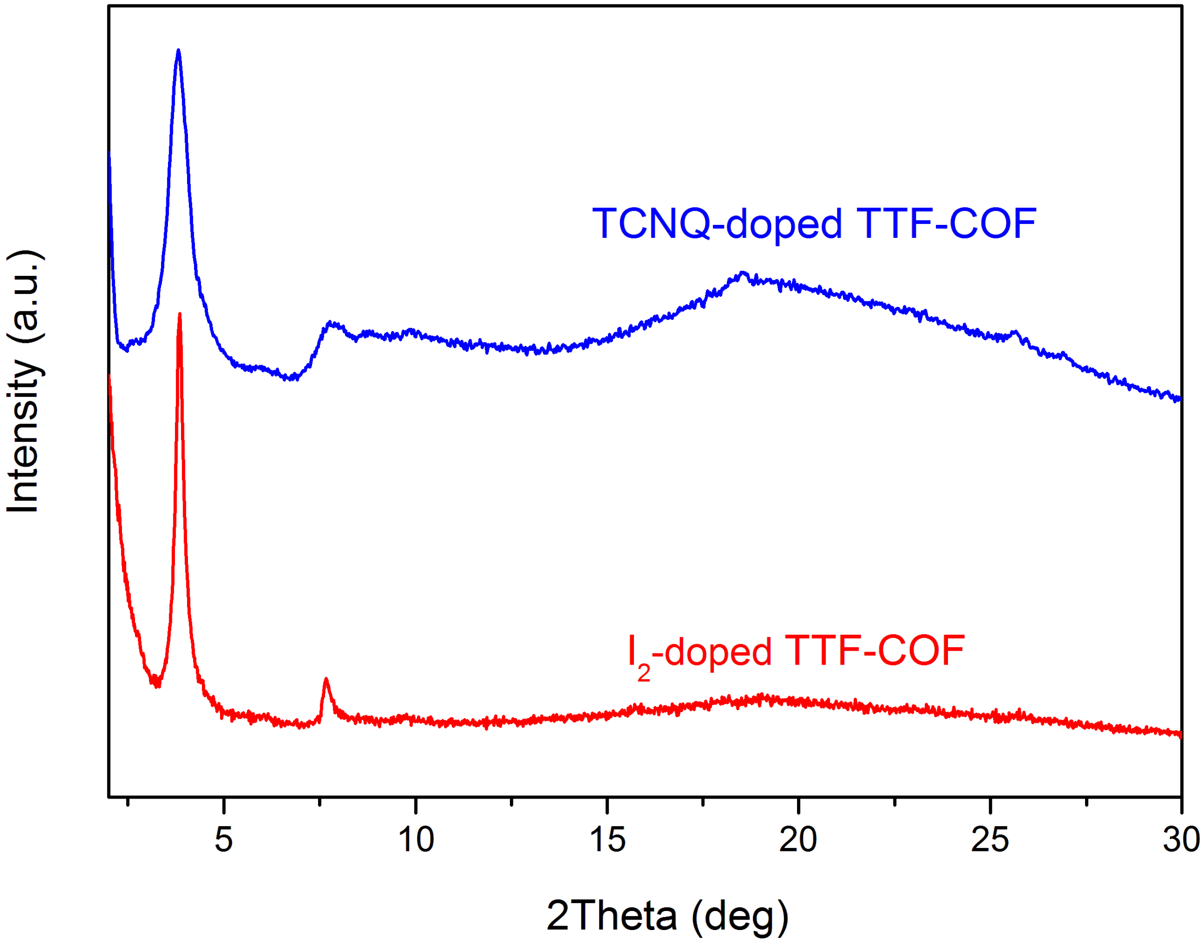

Figure S18. PXRD patterns of I_2-doped TTF-COF and TCNQ-doped TTF-COF.

Section S6 *Nitrogen sorption isotherm curve and pore size distribution*.

Nitrogen adsorption/desorption isotherm was measured using a Tristar II surface area and porosimetry analyzer (Micromeritics, Norcross, GA) and used for the calculation of surface areas.

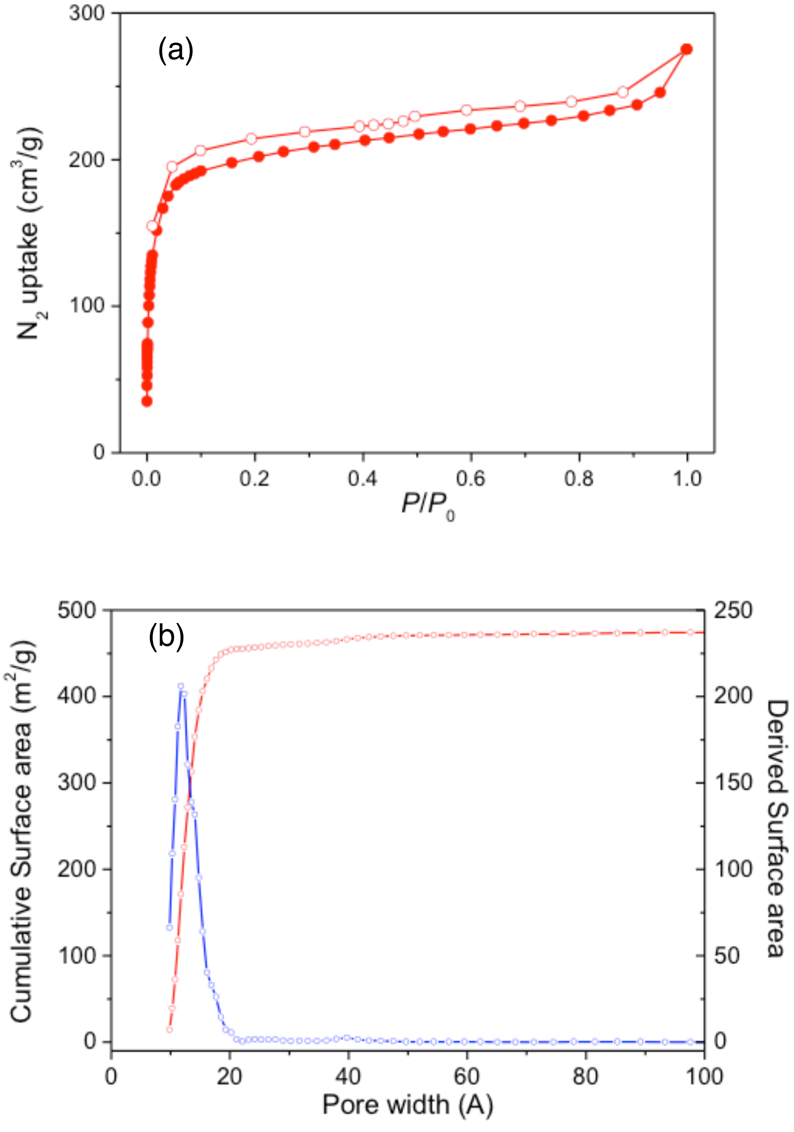

Figure S19. (a) N_2 adsorption (●) and desorption (○) isotherm curves of TTF-COF powder. (b) Pore size distribution of TTF-COF powder.

Section S7. *Thermogravimetric analysis (TGA).*

Thermogravimetric analysis (TGA) was acquired on a TA Instruments Q5000IR TGA-MS with a heating rate of 10 °C/min in flowing argon atmosphere.

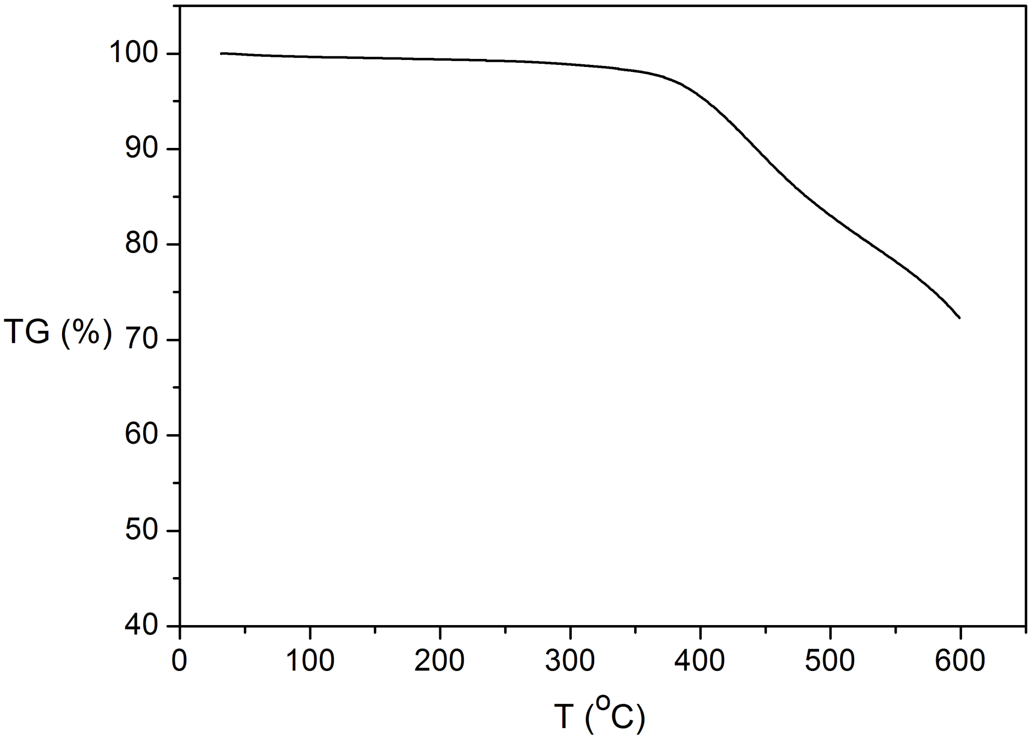

Figure S20. The TGA curve of TTF-COF.

Section S8. *Conductivity measurements*.

Conductivity measurements were taken using a model CPX-HF Lakeshore Probe Station and an Agilent 4155C Semiconductor parameter Analyzer at room temperature and pressure.

Device Fabrication and Testing. Silicon substrates were cut into 16 x 8 mm pieces, and were then cleaned at 40 °C in soap water, DI water, acetone, and isopropanol under subsequent sonication before being dried in an oven at 130 °C for at least one hour. The substrates were then transferred to a thermal evaporator in a nitrogen glovebox where 45 nm of Au was evaporated on top of a 5 nm Cr adhesion layer through a shadow mask, to give a channel width and length of 3 mm and 125 µm, respectively. After the COF film was grown upon the substrate as described below, the sample's conductivity was measured using a two-probe measurement.

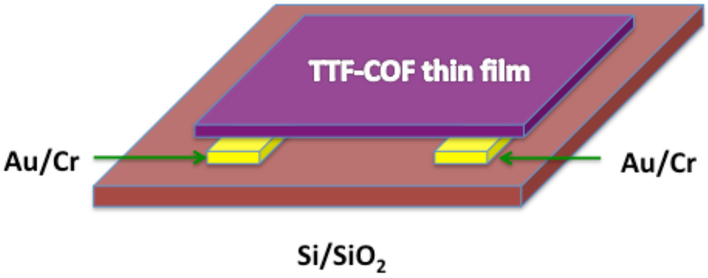

Figure S21. Schematic drawing of the TTF-COF thin film device grown on Si/SiO$_2$ substrate with pre-fabricated Au/Cr electrodes.

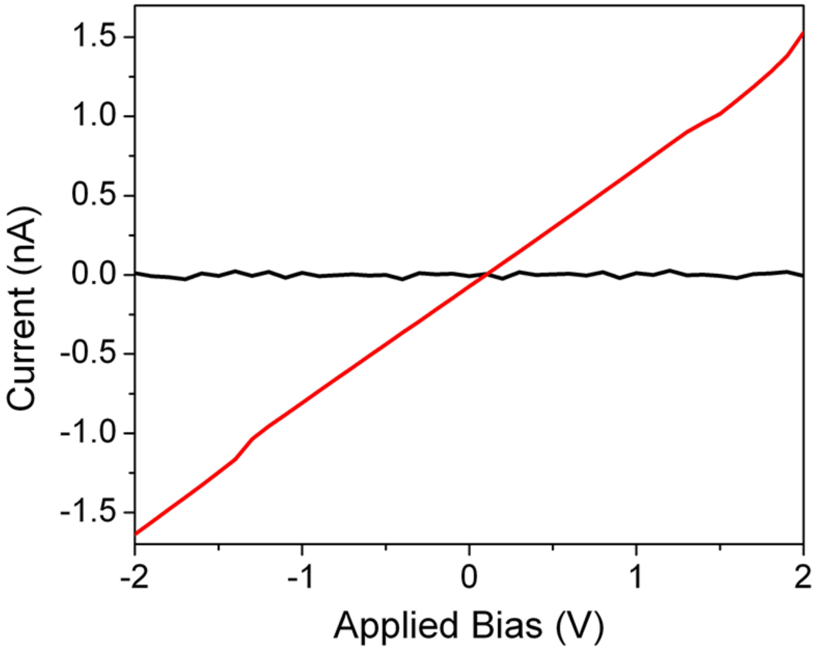

Figure S22. Comparison of the I-V curves of the analog compound **2** (black) and the TTF-COF thin film (red).

Section S9. *UV-vis-near IR (NIR) spectra*.

UV-Vis-NIR spectra were recorded at room temperature using a Cary 5000 UV-Vis-NIR spectrometer.

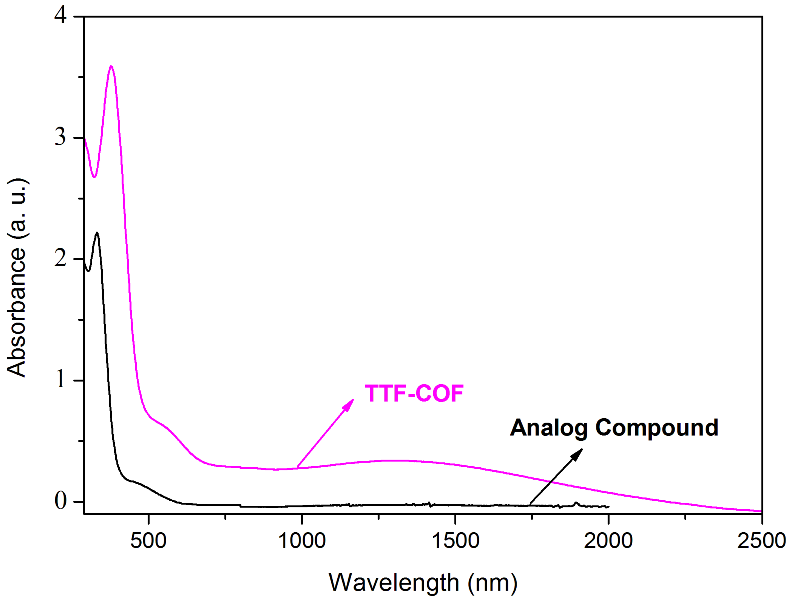

Figure S23. UV-Vis spectra of thin films of the analog compound **2** and TTF-COF.

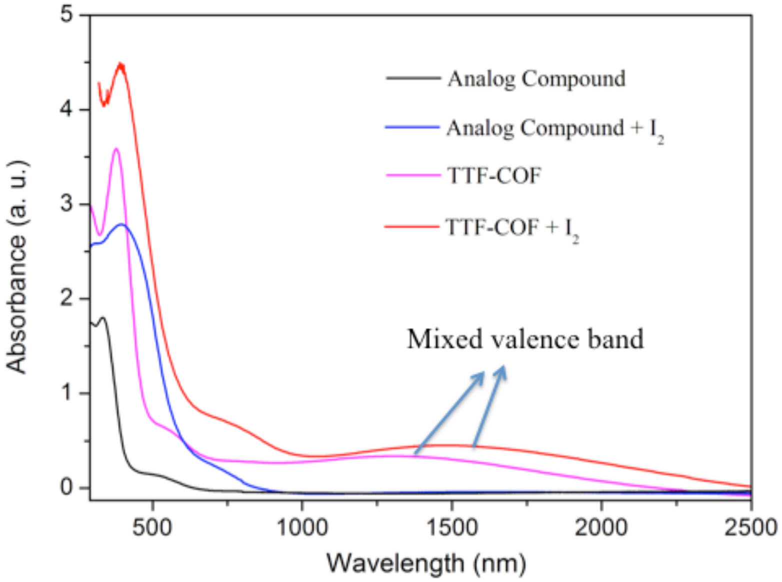

Figure S24. Comparison of the UV-vis-NIR spectra of the pristine thin films of the analog compound and TTF-COF, and the same films after exposure to I_2 for two hours. The mixed-valence band is clearly present in the TTF-COF samples but is absent in the analog compound.

Section S10. *EPR simulation.*

EPR experiments were recorded using a ELEXSYS-II Bruker spectrometer, equipped with a SuperX FT-EPR bridge and a 4102ST universal resonator, at the X-band (~9.8 G) at room temperature under air. Modulation frequency of 100 KHz, modulation amplitude of 5 G, and microwave attenuation of 2 db were employed to ensure the peak resolution and maximum intensity. Modeling of the EPR signals was performed using Matlab toolbox 'EasySpin 4.4.4'. Simulated results for the TTF-COF sample indicate the existence of two types of paramagnetic centers, with a main component of g=2.0065 (97%) and a minor component (3%) with g=2.003. After doping with TCNQ, the EPR spectrum shows hyperfine splitting induced by the two ^{14}N from TCNQ structure, in addition to the g value from TTF$^{\cdot+}$. After I_2 doping, the EPR spectra becomes much stronger and broader, which reveals the formation of TTF-I_2 complex.

Table 3. Spin Hamiltonian Parameters and Abundance of the Radical Species as derived by *Easyspin* Simulation of the Spectra.

	Species	Abundance %	g_{iso}	g_1	g_2	g_3	A_1	A_2	A_3
TTF-COF	A	97	2.0065						
	B	3	2.0030						
TCNQ	A	20	2.0065						
	B	1	2.0030						
	C	79		2.0026	2.0065	2.0086	60	120	10
I_2	A	100		2.007	2.007	2.006			

Section S11. *Proton and carbon nuclear magnetic resonance (^{1}H-NMR and ^{13}C-NMR) spectra.*

Proton and carbon nuclear magnetic resonance (^{1}H-NMR and ^{13}C-NMR) spectra were performed on a Bruker Avance500 II, using the deuterated solvent as lock and tetramethylsilane as an internal standard. All chemical shifts are quoted using the δ scale, and all coupling constants (J) are expressed in Hertz (Hz).

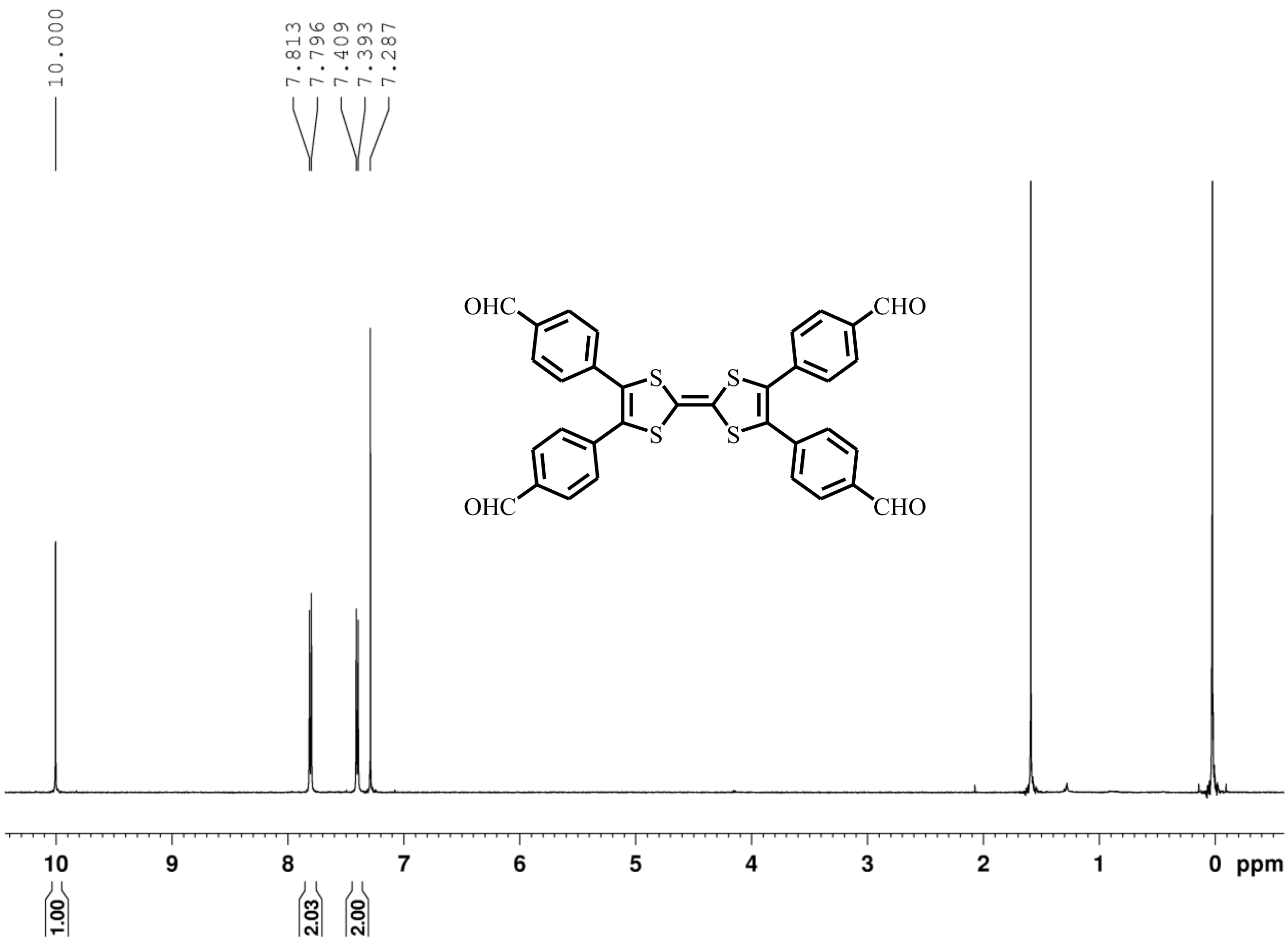

Figure S25. ^{1}H NMR spectrum ($CDCl_3$, 298 K, 500 MHz) of compound **1**.

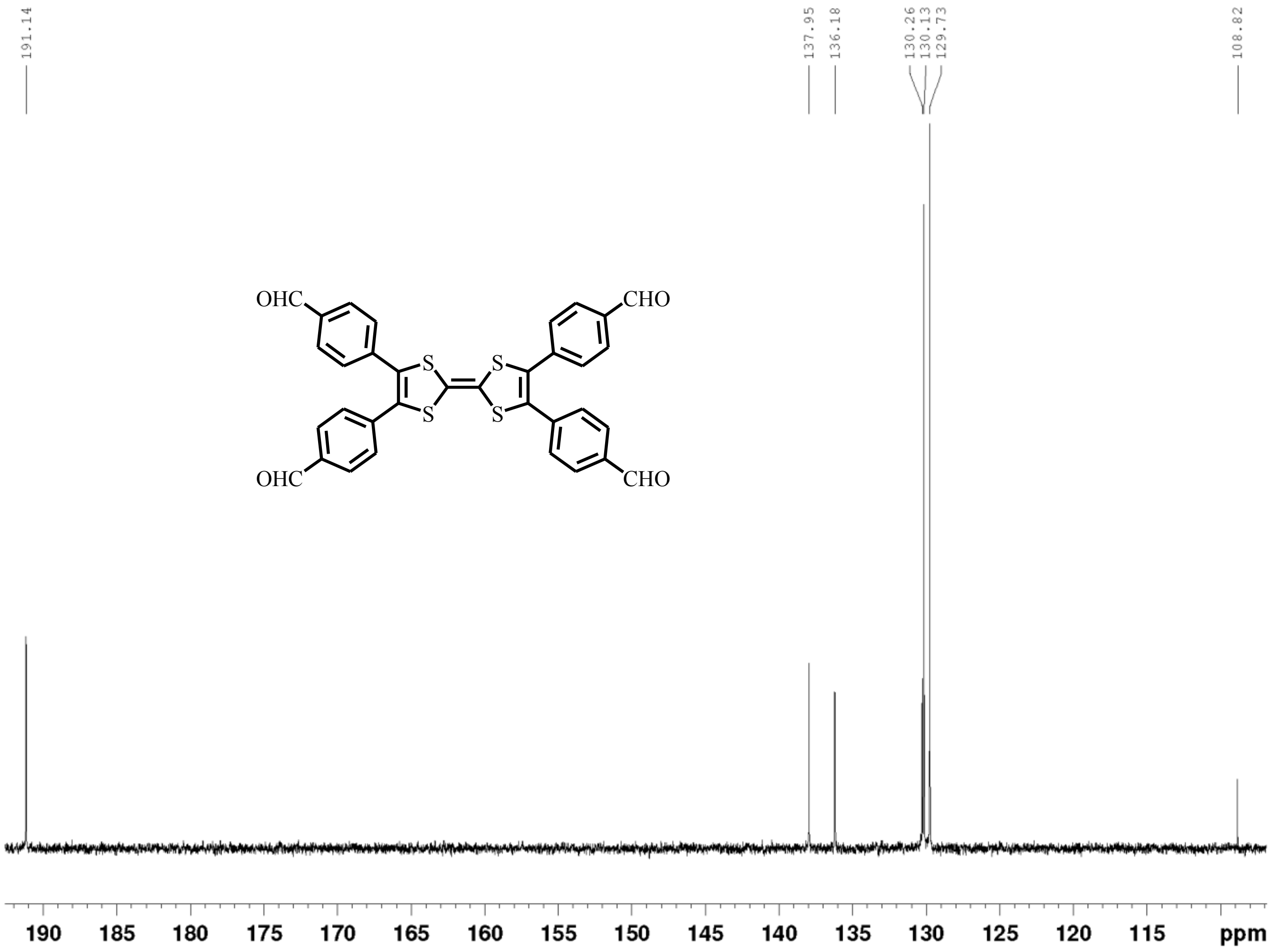

Figure S26. ^{13}C NMR spectrum (CDCl$_3$, 298 K, 125 MHz) of compound **1**.

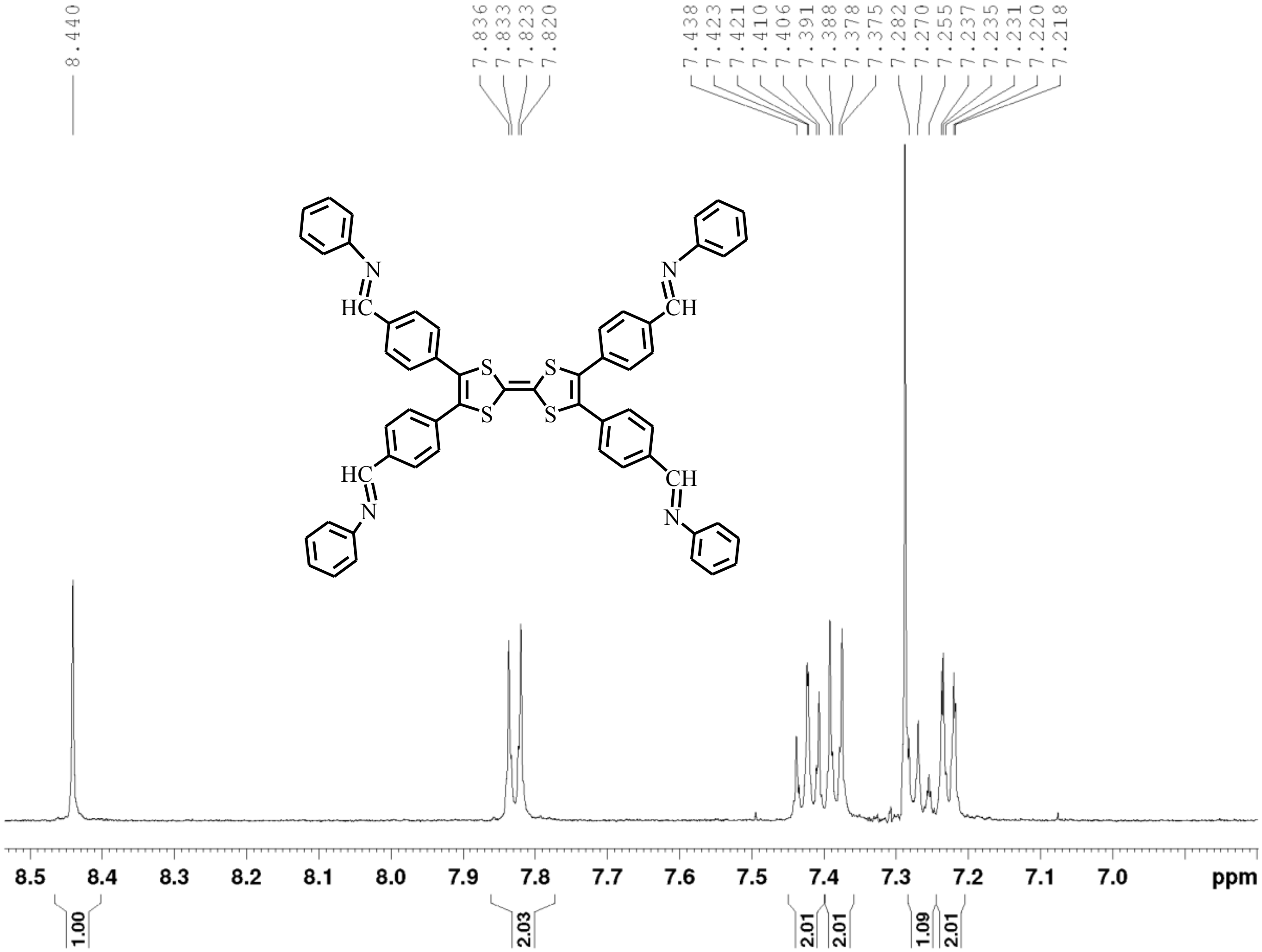

Figure S27. ^{1}H NMR spectrum (CDCl$_3$, 298 K, 500 MHz) of compound **2**.

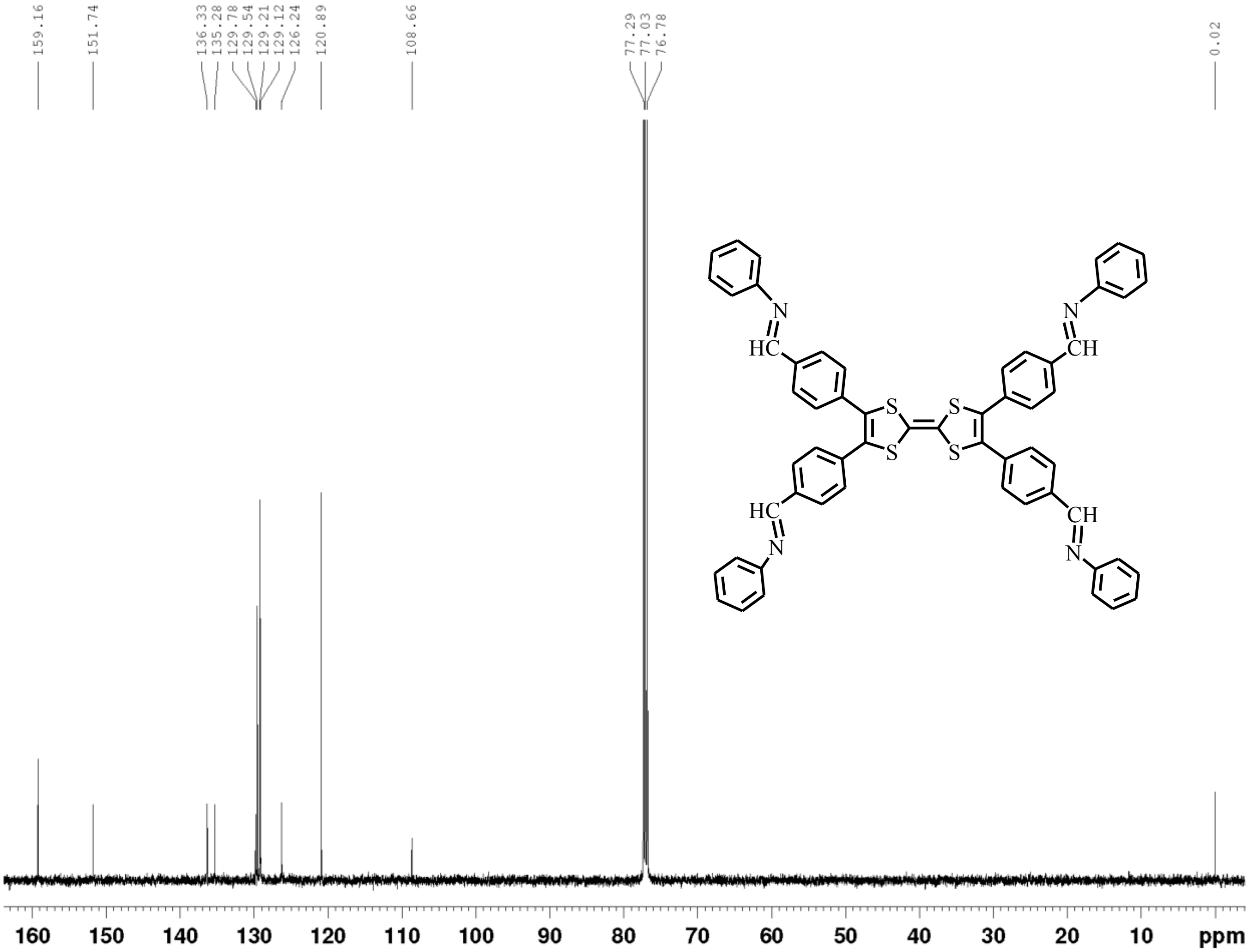

Figure S28. ^{13}C NMR spectrum ($CDCl_3$, 298 K, 125 MHz) of compound **2**.

Section S12. *Matrix-assisted laser desorption ionization (MALDI) mass spectra.*

Matrix-assisted laser desorption ionization (MALDI) mass spectra were measured on 4800 MALDI TOF/TOF analyzer from Applied Biosystems.

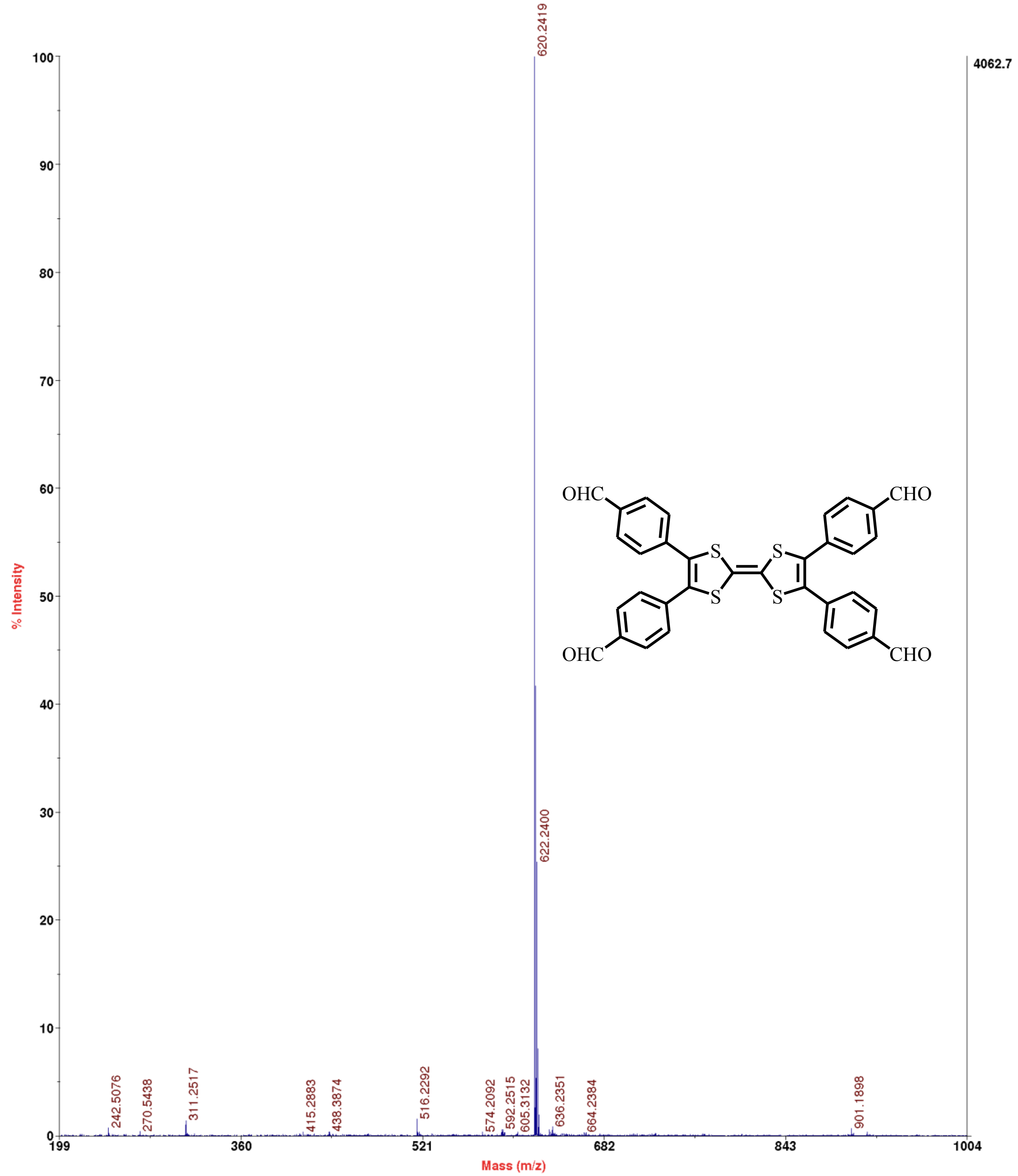

Figure S29. MS (MALDI-TOF) of compound **1**.

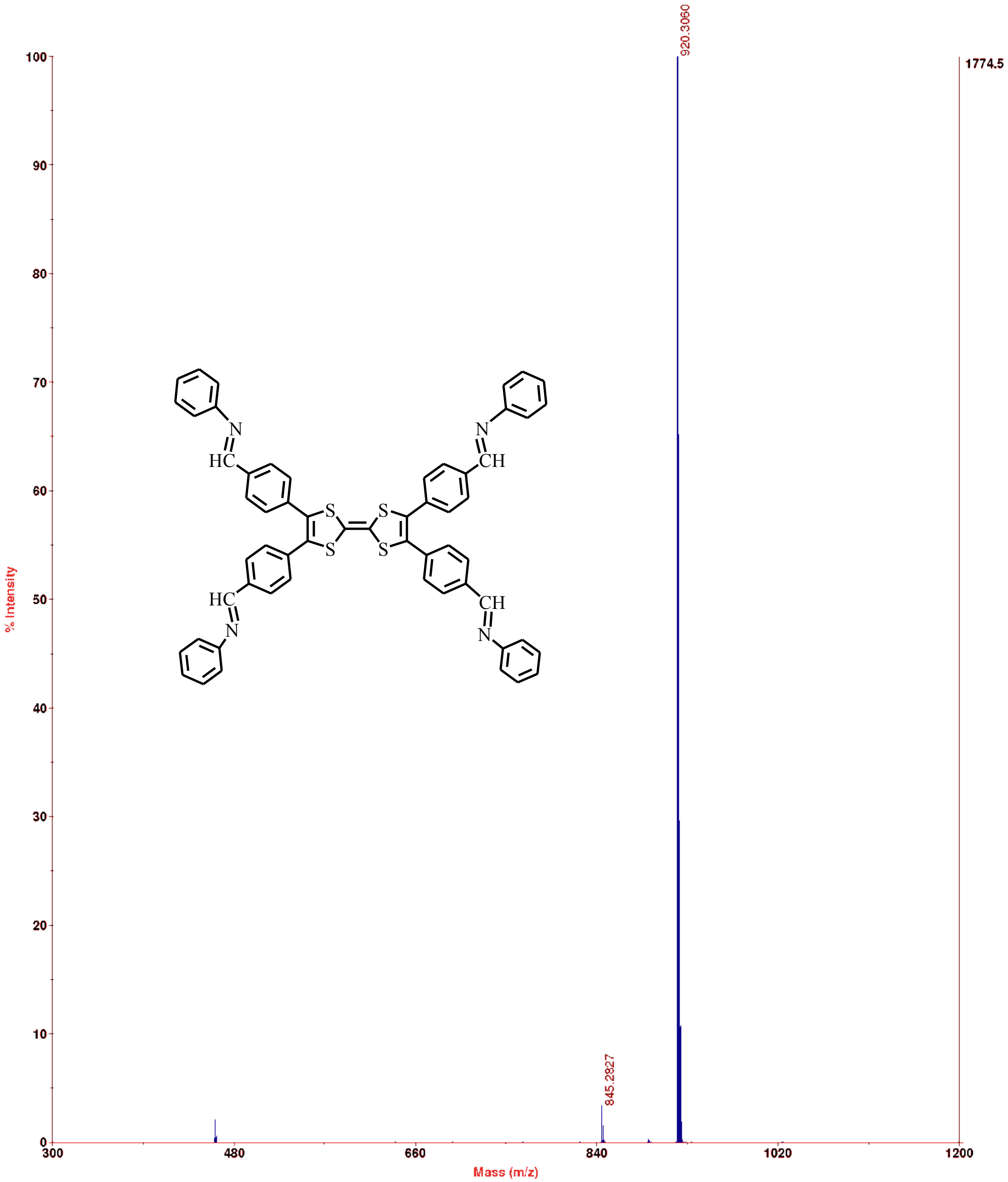

Figure S30. MS (MALDI-TOF) of compound **2**.

References:

(1) *SAINT and APEX 2 Software for CCD Diffractometers*; Bruker AXS Inc.: Madison, WI, USA, **2009**.

(2) Sheldrick, G. M. *Acta Crystallogr.* **2008**, *A64*, 112−122.

(3) Sheldrick, G.M., *SHELXTL User Manual*, version 6.12; Bruker AXS Inc.: Madison, WI, USA, **2001**.

(4) Morcombe, C. R.; Zilm, K. W. *J. Magn. Reson.* **2003**, *162*, 479.

(5) Accelrys Software Inc. *Materials Studio 5.0: Modeling Simulation for Chemical and Material*, San Diego, CA, **2009**.